

Rothamsted Repository Download

A - Papers appearing in refereed journals

Sinhuber, M., Van der Vaart, K., Yenchia, F., Reynolds, A. M. and Ouellette, N.T. 2021. An equation of state for insect swarms. *Scientific Reports*. 11 (3773). <https://doi.org/10.1038/s41598-021-83303-z>

The publisher's version can be accessed at:

- <https://doi.org/10.1038/s41598-021-83303-z>

The output can be accessed at: <https://repository.rothamsted.ac.uk/item/9832x/an-equation-of-state-for-insect-swarms>.

© 12 February 2021, Please contact library@rothamsted.ac.uk for copyright queries.

1 **An equation of state for insect swarms**

2 Michael Sinhuber^{1, #, †}, Kasper van der Vaart^{1, #}, Yenchia Feng¹, Andrew M. Reynolds², and
3 Nicholas T. Ouellette^{1, *}

4
5 ¹Department of Civil and Environmental Engineering, Stanford University, Stanford, CA 94305,
6 USA.

7 ²Rothamsted Research, Harpenden, Hertfordshire, AL5 2JQ, United Kingdom.

8
9 #These authors contributed equally to this work.

10 †Present address: Carl von Ossietzky Universität Oldenburg, 26129 Oldenburg, Germany.

11 *Correspondence: Nicholas T. Ouellette (email: nto@stanford.edu)

12
13 **Collective behaviour in flocks, crowds, and swarms occurs throughout the biological world.**
14 **Animal groups are generally assumed to be evolutionarily adapted to robustly achieve**
15 **particular functions, so there is widespread interest in exploiting collective behaviour for**
16 **bio-inspired engineering. However, this requires understanding the precise properties and**
17 **function of groups, which remains a challenge. Here, we demonstrate that collective groups**
18 **can be described in a thermodynamic framework. We define an appropriate set of state**
19 **variables and extract an equation of state for laboratory midge swarms. We then drive**
20 **swarms through “thermodynamic” cycles via external stimuli, and show that our equation**
21 **of state holds throughout. Our findings demonstrate a new way of precisely quantifying the**
22 **nature of collective groups and provide a cornerstone for potential future engineering design.**
23

24 **Introduction**

25 Organisms on every size scale, from single-celled¹ to highly complex², regularly come together in
26 groups. In many cases, such aggregations are collective, in that the group as a whole displays
27 properties and functionality distinct from those of its individual members or simply their linear
28 sum^{3,4}. It is generally assumed that since evolution has led so many different kinds of animals to
29 behave collectively, the performance of collective groups at whatever task they seek to achieve
30 ought to be well beyond the capabilities of a single individual⁵, while also being robust to uncertain
31 natural environments^{6,7} and operating without the need for top-down control⁸. For these reasons,
32 there has been significant interest both in understanding how collectivity conveys these
33 advantages⁹ and how to exploit it in engineered systems^{10,11}.

34
35 Taking advantage of evolutionary adaptation for the design of such a bio-inspired artificial
36 collective system requires both determining the interaction rules used by real animals and properly
37 understanding the function of the group. Both of these tasks remain a challenge. Extracting
38 interaction rules by observing group behaviour is a highly nontrivial inverse problem¹² that can
39 typically only be solved by assuming a modelling framework *a priori*^{13,14}. Appropriate model
40 selection is made more difficult given that interactions may change in different contexts^{7,8,15}. Even
41 less work has been done to precisely determine the tasks optimized by collective behaviour.
42 Assumptions about the purpose of group behaviour typically come from ecological reasoning¹⁶
43 rather than quantitative empirical evidence⁸—and in some cases, such as hypothesized
44 aerodynamic benefits conveyed to flocking birds, such reasoning has proved to be incorrect^{17,18}.

45

46 We argue that the essential nature of the group functionality is encoded in its properties—and
47 therefore that understanding these properties both allows one to quantify the purpose of the
48 collective behaviour and to predict the response of the group to environmental changes. As recent
49 work has demonstrated¹⁹⁻²¹, a powerful way to characterize these properties is to borrow ideas
50 from other areas of physics. For groups on the move such as human crowds, hydrodynamics is a
51 natural choice, and empirically measured constitutive laws have allowed the formulation of
52 equations of motion that accurately predict how crowds flow²⁰. But for stationary groups such as
53 insect swarms, where the group as a whole does not move even though its constituent individuals
54 are continuously rearranging, thermodynamics is a more natural framework, as it allows one to
55 precisely describe the state of the system irrespective of its net motion²². The most fundamental
56 relationship for doing so is the equation of state, which links the state variables that describe the
57 macroscopic properties of the system and encodes how they co-vary in response to environmental
58 changes.

59
60 Here, we formulate such an equation of state for laboratory swarms of the non-biting midge
61 *Chironomus riparius* (Fig. 1a). We define appropriate state variables, and empirically deduce their
62 relationship by analysing a large data set of measured swarms²³. Then, by applying a suitable
63 sequence of external perturbations to the swarms, we show that we can drive them through a
64 thermodynamic cycle in pressure–volume space throughout which our empirical equation of state
65 holds.

66
67
68

69 **Results**

70 **State variables.** The first step in describing the macroscopic properties of the swarm is to define
71 a set of state variables that fully characterizes the state of the system. The equation of state then
72 links these state variables in a functional relation. In classical thermodynamics, a complete set of
73 state variables is given by the conjugate pairs of pressure P and volume V , temperature T and
74 entropy S , and, if the number of particles is not fixed, chemical potential μ and number of particles
75 N . We use an analogous set of state variables here to characterize swarms. The most
76 straightforward state variable to define is the number of individuals N , which is given simply by
77 the number of midges ~~that are participating in the swarm at a given time~~ (note that midges that are
78 ~~not swarming simply sit on the walls or floor of the laboratory enclosure~~). The volume V of the
79 swarm can be straightforwardly defined and computed as the volume of the convex hull enclosing
80 all the midges. Note that, while N and V are not independently controllable quantities, the ratio
81 N/V is empirically approximately constant in large swarms²⁵, meaning that the “thermodynamic”
82 limit (that is, $N \rightarrow \infty$ and $V \rightarrow \infty$ with $\frac{N}{V} \rightarrow \rho$) is approached in our swarms³³. In typical swarming
83 events, N changes on a time scale that is very slow compared to the swarm dynamics; thus, a
84 chemical potential is not needed to describe the instantaneous state of the swarm. Note, though,
85 that since the number of midges varies between measurements that may be separated by many
86 days, N remains a relevant state variable for capturing swarm-to-swarm variability.

87
88 The remaining three state variables are somewhat more subtle, but can be defined by building on
89 previous work. It has been explicitly shown²⁴ that a virial relation based on the kinetic energy and
90 an effective potential energy holds for laboratory swarms of *Chironomus riparius*. For particles
91 moving in a potential, this virial relation can be used to define a pressure²⁴. As we have shown

92 previously, swarming midges behave as if they are trapped in a harmonic potential well that binds
 93 them to the swarm, with a spring constant $k(N)$ that depends on the swarm size^{24,25} (Fig. 1b). The
 94 difference between the kinetic energy and this harmonic potential energy thus allows us to compute
 95 a pressure^{4,24,26}, which is conceptually similar to the swim pressure defined in other active
 96 systems²⁷. The virial theorem thus provides a link between kinetic energy, potential energy, and a
 97 field that plays the role of a pressure, when coupled with the observation that individual midges to
 98 a good approximation behave as if they are moving in a harmonic potential^{24,25}. We can write this
 99 virial pressure P (per unit mass, assuming a constant mass per midge) as

$$100 \quad P = \frac{1}{3NV} \sum_{i=1}^N \left(v_i^2 - \frac{1}{2} \langle k \rangle r_i^2 \right),$$

101 where N is the number of midges in the swarm, V is the swarm volume, v_i is the velocity of midge
 102 i , r_i is its distance from the swarm centre of mass, and $\langle k \rangle = \langle -\mathbf{a}_i \cdot \hat{\mathbf{r}}_i / r_i \rangle$ is the effective
 103 spring constant of the emergent potential well that binds midges to the swarm. In this expression,
 104 \mathbf{a}_i is the acceleration of midge i , $\hat{\mathbf{r}}_i$ is the unit vector pointing from a midge towards the centre of
 105 mass of the swarm (defined as given by $1/N \sum_{i=1}^N \mathbf{r}_i$) and averages are taken over the individuals
 106 in the swarm. This spring constant depends on the swarm size N (Fig. 1b). We note that we have
 107 previously simply used the directly computed potential energy $-\langle \mathbf{a}_i \cdot \mathbf{r}_i \rangle$ to define the
 108 pressure^{4,26}; here, we instead average the potential terms and fit them to a power law in N (Fig. 1b)
 109 to mitigate the contribution of spurious instantaneous noise in the individual accelerations
 110 ~~positions that arises would be enhanced by differentiating them twice to compute accelerations due~~
 111 ~~to the second-order differentiation in determining the accelerations.~~ We use this power law to
 112 determine the spring constant k instantaneously at each time step.

113

114 The results from the two methods for computing the pressure are similar and consistent, but the
115 method we use here is less prone to noise. Physically, this pressure P can be interpreted as the
116 additional, spatially variable energy density required to keep the midges bound to the swarm given
117 that their potential energy varies in space but their mean velocity (and therefore kinetic energy)
118 does not. Thus, compared to a simple passive particle moving in a harmonic well, midges have
119 more kinetic energy than expected at the swarm edges; this pressure compensates for the excess
120 kinetic energy. This pressure should be viewed as a manifestation of the active nature of the midges
121 (similar to a swim pressure²⁷), since the kinetic energy is an active property of each individual
122 midge and the potential energy is an emergent property of the swarm.

123

124 We can define a Shannon-like entropy S via its definition in terms of the joint probability
125 distributions of position and velocity. This entropy is defined as

126
$$S = - \int_{-\infty}^{\infty} p(x,v) \log_2 p(x,v) dx dv,$$

127 where $p(x,v)$ is the joint probability density function (PDF) of midge position and velocity. S here
128 is measured in bits, as it is naturally an information entropy. Empirically, we find that the position
129 and velocity PDFs are nearly statistically independent for all components and close to Gaussian,
130 aside from the vertical component of the position (Fig. 1c-f). However, the deviation from
131 Gaussianity in this component (which occurs because of the symmetry breaking due to the ground)
132 does not significantly affect the estimate of the entropy; thus, we approximate it as Gaussian as
133 well. Making these approximations, we can thus analytically write the (extensive) entropy as

134
$$S = \frac{3N}{\ln 2} \ln (2N\pi e \sigma_x \sigma_v),$$

135 where σ_x and σ_v are the standard deviations of the midge positions and velocities, respectively. In
 136 practice, we calculated σ_v by averaging the instantaneous root-mean-square values of all three
 137 velocity components rather than a time-averaged value; the difference between these components
 138 was always less than 10%. This expression makes it more clear why the Gaussian approximation
 139 for the vertical component of the position is reasonable here: only the mean and variance of the
 140 PDFs are required to compute the entropy, and these low moments are very similar for the true
 141 data and the Gaussian estimate.

142 Although there is no obvious definition of temperature for a swarm, we can define one
 143 starting from the entropy, since temperature (when scaled by a Boltzmann constant) can be defined
 144 as the increase in the total physical energy of the system due to the addition of a single bit of
 145 entropy. Given our definitions, adding a single bit of entropy (that is, setting $S \rightarrow S + 1$) for
 146 constant σ_x and N (that is, a swarm of fixed number and spatial size) is equivalent to setting $\sigma_v \rightarrow$
 147 $2^{1/(3N)}\sigma_v$. Adding this entropy changes the total energy of the system by an amount

$$148 \quad \frac{3}{2}\sigma_v^2 N \left(2^{\frac{2}{3N}} - 1 \right) \equiv k_B^* T,$$

149 which we thus define as the temperature $k_B^* T$. Even though this temperature is nominally a
 150 function of the swarm size N , it correctly yields an intensive temperature as expected in the limit
 151 of large N , as the explicit N -dependence vanishes in that limit since $\lim_{N \rightarrow \infty} k_B^* T = \sigma_v^2 \ln 2$. In
 152 practice, this limit is achieved very rapidly: we find that this temperature is nearly independent of
 153 N for N larger than about 20, consistent with our earlier results on the effective “thermodynamic
 154 limit” for swarms³³. The effective Boltzmann constant k_B^* is included here to convert between
 155 temperature and energy, though we note that we cannot set its value, as there is no intrinsically
 156 preferred temperature scale.

157

158 **Equipartition.** With these definitions in hand, we can evaluate the suitability of these quantities
159 for describing the macroscopic state of midge swarms. First, we note that proper state variables
160 ought to be independent of the swarm history; that is, they ought to describe only the current state
161 of the system rather than the protocol by which that state was prepared. Although this property is
162 difficult to prove incontrovertibly, none of the definitions of our state variables have history
163 dependence. We further find that when these state variables are modulated (see below), their
164 correlation times are very short, lending support to their interpretation as true state variables. We
165 can also compare the relationships between these state variables and the swarm behaviour to what
166 would be expected classically. In equilibrium thermodynamics, for example, temperature is
167 connected to the number of degrees of freedom (d.o.f.) in a system via equipartition, such that each
168 d.o.f. contributes an energy of $\frac{1}{2}k_B^* T$. We can write the total energy E of a swarm as the sum of
169 the kinetic energy $E_k(t) = \frac{1}{2}v^2$ and potential energy $E_p(t) = \frac{1}{2}k(N)r(t)^2$ for all the individuals,
170 where r is the distance of a midge to the swarm centre of mass, v is the velocity of a midge, and
171 $k(N)$ is the effective spring constant. Surprisingly, even though individual midges are certainly not
172 in equilibrium due to their active nature, we find that the total energy is linear in both T and N (Fig.
173 2a), and that there is no apparent anisotropy, suggesting that equipartition holds for our swarms.
174 This result is highly nontrivial, especially given that our definition of T does not contain the spring
175 constant $k(N)$, which is only determined empirically from our data. Moreover, the slope of the $E/$
176 $k_B^* T$ curve is well approximated as $(9/2)N$, implying that each midge has 9 effective d.o.f. (or 6
177 after discounting the factor of $\ln 2$ in our definition of $k_B^* T$) These d.o.f. can be identified as 3
178 translational and 3 potential modes, given that the potential well in which the midges reside is
179 three-dimensional. These results demonstrate the surprising applicability of equilibrium
180 thermodynamics for describing the macroscopic state of swarms²⁸.

181

182 **Equation of state.** The fundamental relation in any thermodynamic system is the equation of state
183 that expresses how the state variables co-vary. Equations of state are thus the foundation for the
184 design and control of thermodynamic systems, because they describe how the system will respond
185 when a subset of the state variables are modulated. Any equation of state can be written in the form

186 $P = f(V, T, N)$ for some function f . Although the form of f is *a priori* unknown, it can typically
187 be written as a power series in V , T , and N , in the spirit of a virial expansion. We fit the equation
188 of state to our data assuming the functional form

$$189 \quad P = f(V, k_B^* T, N) = c_4 V^{c_1} (k_B^* T)^{c_2} N^{c_3},$$

190 and using non-linear least-squares regression. We chose to fit to the pressure for convenient
191 analogy with a thermodynamic framework, but any other variable would have been an equivalent
192 possibility. We note that when fitting, we normalized all the state variables by their root-mean-
193 square values so that they were all of the same order of magnitude. These normalization pre-factors
194 do not change the exponents, but are instead simply absorbed into c_4 . Thus, to leading order, we
195 assume $P = f(V, k_B^* T, N) \propto V^{c_1} (k_B^* T)^{c_2} N^{c_3}$ and fit this relation to the swarm pressure (Fig.
196 2B,C), obtaining $c_1=-1.7$, $c_2=2$, and $c_3=1$, with uncertainties on the order of 1%. Although the
197 expression for the pressure does depend on three parameters [in a nonlinear fashion](#), the resulting
198 estimates for these parameters are remarkably stable and consistent across all measurements.
199 Hence, we arrive at the equation of state $PV^{1.7} \propto N(k_B^* T)^2$.

200
201 This equation of state reveals aspects of the nature of swarms, particularly when compared with
202 the linear equation of state for an ideal gas (where $PV = Nk_B T$). In both cases, for example, to
203 maintain a fixed pressure and volume, smaller systems need to be hotter; but this requirement is
204 less severe for swarms since the temperature is squared, meaning that midges have to speed up
205 less than ideal gas molecules do. Likewise, to maintain a fixed temperature, volume expansion
206 must be counteracted by a reduction in pressure; but midges must lower the pressure more than a
207 corresponding ideal gas, which is reflective of the decrease of the swarm spring constant with size.

208

209 **Thermodynamic cycling.** Beyond such reasoning, however, the true power of an equation of state
210 in thermodynamics lies in specifying how the state variables will change when some are varied
211 but the system remains in the same state, such as in an engine. To demonstrate that our equation
212 of state similarly describes swarms, it is thus necessary to drive them away from their natural state.
213 Although it is impossible to manipulate the state variables directly in this system of living
214 organisms as one would do with a mechanical system, we have shown previously that time-varying
215 acoustic²⁹ and illumination²⁶ stimulation lead to macroscopic changes in swarm behaviour. Here
216 we therefore build on these findings and use interlaced illumination changes and acoustic signals
217 to drive swarms along four distinct paths in pressure-volume space, analogous to a thermodynamic
218 engine cycle. The stimulation protocol is sketched in Fig. 3a. The “on” state of the acoustic signal
219 is telegraph noise (see Experimental details), while the “off” state is completely quiet. The
220 illumination signal simply switches between two different steady light levels. Switching between
221 the four states of “light-high and sound-on,” “light-high and sound-off,” “light-low and sound-
222 off,” and “light-low and sound-on” with a 40-second period (Fig. 3a) produces the pressure-
223 volume cycle shown in Fig. 3b. We suspect that the loops in the cycle stem from the swarm’s
224 typical “startle” response after abrupt changes in environmental conditions, followed by a rapid
225 relaxation to a steady state^{26,29}.

226
227 In addition to the pressure and volume, we can also measure the other state variables as we perturb
228 the swarms. Given that we do not observe any evidence of a phase transition, we would expect
229 that our equation of state, if valid, should hold throughout this cycle. To check this hypothesis, we
230 used the measured V , T , and N values during unperturbed experiments along with the equation of
231 state to predict the scaling exponents, and in turn the pressure P . We then use these baseline,

232 unperturbed exponents and V , T , and N during the interlaced perturbations to predict a pressure P .
233 This pressure prediction matches the measured signal exceptionally well (Fig. 3c,d) even though
234 the equation of state was formulated only using data from unperturbed swarms, highlighting the
235 quality of this thermodynamic analogy. Although we might expect that a strong enough
236 perturbation might lead to qualitatively different behaviour (if the swarm went through the analog
237 of a phase transition), our results give strong support to the hypothesis that our equation of state
238 should hold for any perturbation that does not drive such a transition.

Commented [NTO1]: Maybe cite the Italian PRL on swarm criticality?

240 Discussion

241 Our findings demonstrate the surprising efficacy of classical equilibrium thermodynamics
242 for quantitatively characterizing and predicting collective behaviour in biology. Even though
243 individual midges are certainly not in equilibrium and need not obey the same rules as, for
244 example, particles in an ideal gas, we find that the collective behaviour of ensembles of these
245 individuals is surprisingly simple. The existence of a well-defined equation of state for this system
246 gives us a new way both of illuminating the purpose of collective behaviour, given that it encodes
247 the nature of the collective state, and quantitatively distinguishing different kinds of animal groups
248 that may have similar movement patterns but different functions^{1,2,3,8}. Importantly, we note that
249 this equation of state is not a swarm model per se, in that it does not make any detailed predictions
250 about the dynamics of individuals. Rather, it gives us a quantitative way of analysing and
251 interpreting swarm data at the macroscale. ~~In contrast to studies that rely on modelling the~~
252 individuals behavioural rules, our findings opens a path to a more general description of collective
253 behaviour.—Finally, these results also provide a natural starting point for designing artificial
254 collective systems by outlining a framework for adapting intuition and expertise gained from

Commented [NTO2]: I don't think I agree with the comment you added. Our work isn't really in contrast to rule-based models at all; indeed, I think it should be possible to implement our analysis on the results of those models! It's really more about the level of description (e.g., macro vs. micro).

255 engineering thermodynamic systems to this new situation. This approach could, for example, be
256 useful to guide the design of engineered drone swarms via machine learning techniques³⁴⁶ and to
257 provide a precise and quantifiable global ~~properties that included~~ description of the collective nature
258 of swarms.

259

260 **Methods**

261 In our laboratory we maintain a colony of *C. riparius* midges in an (122cm)³ acrylic tank. *C.*
262 *riparius* larvae develop in eight 10 litre breeding tanks filled with dechlorinated, aerated water and
263 a cellulose substrate. The colony is regulated on an artificial circadian rhythm with 16 hours of
264 light and 8 hours of night using an overhead light on a timer. Over the roughly 2-week life cycle
265 of the midges, larvae become pupae and eventually mature into flying adult midges. Females in
266 the colony mate with males, fertilizing eggs that they lay in the breeding tanks, thus closing the
267 life cycle.

268

269 Just after dusk and dawn, male midges will form mating swarms over ground-based visual features
270 known as swarm markers³⁰. In our laboratory, this feature is a black square plate. Swarms are
271 consistently spheroidal with a swarm diameter that depends on the number of swarming
272 individuals²⁵. Typical swarm sizes in our laboratory range from 10 to 100 individuals. Note that
273 individuals that are not participating in the swarm do not fly; rather, they sit on the walls or floor
274 of the enclosure. The swarm behaviour is recorded by three cameras placed outside the enclosure.

275

276 The cameras used to image the swarms were hardware-synchronized Point Grey Flea3 1.3 MP
277 Mono USB3 Vision cameras running at 100 frames per second, synchronized via an external

278 function generator. To illuminate the midges without interfering with their natural behaviour, we
279 used 20 3W near-infrared LED arrays placed on top of and inside the measurement tank. *C.*
280 *riparius* do not see in the infrared, but it is detectable by the cameras, thus allowing non-intrusive
281 imaging of the swarming events. The cameras were placed on tripods outside the midge enclosure,
282 and were arranged in a horizontal plane with angular separations of 30 and 70 degrees²³ and placed
283 far enough from the experimental enclosure to ensure that the full swarm was always fully within
284 the field of view of each camera. Calibration of the imaging system was done via Tsai's method³¹,
285 using a flat plate with a regular dot pattern placed inside the tank (and removed before the initiation
286 of swarming) as a calibration reference. During each acquisition session, each of which typically
287 occurred on different days, we recorded between 30000 and 100000 frames of data, corresponding
288 to 5 minutes to 16 minutes and 40 seconds of swarming. To obtain three-dimensional trajectories
289 from the individual camera recordings, we first processed each image to obtain 2D midge positions
290 in each camera's frame of reference, matched the data between the cameras to obtain 3D midge
291 positions for every midge in the swarm, and finally tracked all the 3D positions in time. The
292 observed swarms are dilute. Even in statistically unusual cases of close midge encounters,
293 individuals can still be identified²³. To process the images, we first removed the background
294 illumination field (obtained by averaging over the full image sequence) and then detected midges
295 simply by computing the centroids of connected regions that were brighter than an empirically set
296 threshold and larger than a minimal pixel size. Regions that were highly non-spherical and very
297 large indicated the overlap of the images of multiple midges in the camera's field of view, and so
298 were split into multiple midges (see ref. 23). The 2D midge coordinates were stereo-matched
299 between the cameras by projecting the lines of sight connecting each camera's centre of projection
300 and each midge's 2D location into 3D space using the calibrated camera model and then

301 identifying near-intersections. In principle, two cameras are sufficient for this purpose, but
302 additional cameras have been shown to significantly improve the confidence and yield of this
303 procedure³². To connect the 3D positions temporally and create trajectories, we used a multi-frame
304 predictive tracking algorithm^{23,32}. Velocities and acceleration were then computed by
305 differentiating the trajectories in time²³. At each time-step, we additionally removed midges that
306 were sitting or walking on the walls or marker rather than flying, identifying them based on a 100-
307 frame moving average of their speed. If this average speed at a given time step was less than 60
308 mm/s, we discarded the individual at that time-step.

309
310 In this study, we applied interleaved perturbations of two different classes to the swarms in
311 conjunction to the observation of unperturbed swarming events. For the first perturbation type, we
312 induced illumination perturbations, generated by a 6500 K Luxeon Star LED array mounted above
313 the midge enclosure, as described in ref. 26. For this study, we modulated the brightness of the
314 LED between 1.4 lux and 2.4 lux, switching every 20 seconds for a period of 40 seconds. A second
315 class of perturbations were acoustic signals that were generated by a small (~5 cm) omnidirectional
316 speaker placed on the swarm marker. We alternated between a quiet state (that is, no sound played
317 through the speaker) and playback of a telegraph noise acoustic signal, again with a 40-second
318 period. This corresponds to up to 25 full cycles per acquisition session. The telegraph noise was
319 constructed by passing a white-noise signal through a low-pass 700 Hz filter, and then playing
320 short pulses of this signal during the acoustic “on” state with varying length and amplitude. We
321 empirically found that filtering the white-noise signal was necessary to induce a persistent response
322 of the swarm. This may be due to swarms’ tendency to adapt to and ignore static changes in their
323 environment while responding persistently to dynamic changes^{26,35}. ~~might potential be connected~~

324 to the intrinsic sound of the wingbeat frequency of male *Chironomus riparius* of 575Hz^{34,35}. The
325 pulse length ranged from 0.1s to 0.3s and the pause between pulses ranged from 0.25s to 0.5s. The
326 noise amplitude was clearly audible over the ambient sound levels in the laboratory, and we varied
327 it only slightly.

328

329

330

331 **References**

- 332 (1) Gregor, T., Fujimoto, K., Masaki, N. & Sawai, S. The onset of collective behavior in social
333 amoebae. *Science* **328**, 1021-1025 (2010).
- 334 (2) Couzin, I. D. & Krause, J. Self-organization and collective behavior in vertebrates. *Adv. Stud.*
335 *Behav.* **32**, 1-75 (2003).
- 336 (3) Sumpter, D. J. T. The principles of collective animal behaviour. *Phil. Trans. R. Soc. B* **361**, 5-
337 22 (2006).
- 338 (4) Sinhuber, M. & Ouellette, N. T. Phase coexistence in insect swarms. *Phys. Rev. Lett.* **119**,
339 178003 (2017).
- 340 (5) Parrish, J. K. & Edelstein-Keshet, L. Complexity, pattern, and evolutionary trade-offs in
341 animal aggregation. *Science* **284**, 99-101 (1999).
- 342 (6) Berdahl, A., Torney, C. J., Ioannou, C. C., Faria, J. J. & Couzin, I. D. Emergent sensing of
343 complex environments by mobile animal groups. *Science* **339**, 574-576 (2013).
- 344 (7) King, A. J., Fehlmann, G., Biro, D., Ward, A. J. & Fürtbauer, I. Re-wilding collective
345 behaviour: an ecological perspective. *Trends Ecol. Evol.* **33**, 347-357 (2018).
- 346 (8) Gordon, D. M. The ecology of collective behavior. *PLoS Biol.* **12**, e1001805 (2014).

347 (9) Couzin, I. D. Collective cognition in animal groups. *Trends Cogn. Sci.* **13**, 36-43 (2009).

348 (10) Rubenstein, M., Cornejo, A. & Nagpal, R. Programmable self-assembly in a thousand-robot
349 swarm. *Science* **345**, 795-799 (2014).

350 (11) Li, S., Batra, R., Brown, D., Chang, H.-D., Ranganathan, N., Hoberman, C., Rus, D. &
351 Lipson, H. Particle robotics based on statistical mechanics of loosely coupled components.
352 *Nature* **567**, 361-365 (2019).

353 (12) Lukeman, R., Li, Y.-X. & Edelstein-Keshet, L. Inferring individual rules from collective
354 behavior. *Proc. Natl. Acad. Sci. U.S.A.* **107**, 12576-12580 (2010).

355 (13) Sumpter, D. J. T., Mann, R. P. & Perna, A. The modelling cycle for collective animal
356 behaviour. *Interface Focus* **2**, 764-773 (2012).

357 (14) Mann, R. P., Perna, A., Strömbom, D., Garnett, R., Herbert-Read, J. E., Sumpter, D. J. T. &
358 Ward, A. J. W. Multi-scale inference of interaction rules in animal groups using Bayesian model
359 selection. *PLoS Comput. Biol.* **9**, e1002961 (2013).

360 (15) Ling, H., McIvor, G. E., Westley, J., van der Vaart, K., Vaughan, R. T., Thornton, A. &
361 Ouellette, N. T. Behavioural plasticity and the transition to order in jackdaw flocks. *under review*
362 (2019).

363 (16) Hamilton, W. D. Geometry for the selfish herd. *J. Theor. Biol.* **31**, 295-311 (1971).

364 (17) Usherwood, J. R., Stavrou, M., Lowe, J. C., Roskilly, K. & Wilson, A. M. Flying in a flock
365 comes at a cost in pigeons. Flying in a flock comes at a cost in pigeons. *Nature* **474**, 494-497
366 (2011).

367 (18) Ling, H., McIvor, G. E., van der Vaart, K., Vaughan, R. T., Thornton, A. & Ouellette, N. T.
368 Costs and benefits of social relationships in the collective motion of bird flocks. *Nat. Ecol. Evol.*
369 **3**, 943-948 (2019).

370 (19) Tennenbaum, M., Liu, Z., Hu, D. & Fernandez-Nieves, A. Mechanics of fire ant
371 aggregations. *Nat. Mater.* **15**, 54-59 (2016).

372 (20) Bain, N. & Bartolo, D. Dynamic response and hydrodynamics of polarized crows. *Science*
373 **363**, 46-49 (2019).

374 (21) van der Vaart, K., Sinhuber, M., Reynolds, A. M. & Ouellette, N. T. Mechanical
375 spectroscopy of insect swarms. *Sci. Adv.* **5**, eeaw9305 (2019).

376 (22) Ouellette, N. T. The most active matter of all, *Matter* **1**, 291-299 (2019).

377 (23) Sinhuber, M., van der Vaart, K., Ni, R., Puckett, J. G., Kelley, D. H. & Ouellette, N. T.
378 Three-dimensional time-resolved trajectories from laboratory insect swarms. *Sci. Data* **6**, 190036
379 (2019).

380 (24) Gorbonos, D., Ianculescu, R., Puckett, J. G., Ni, R., Ouellette, N. T. & Gov, N. S. Long-
381 range acoustic interactions in insect swarms: an adaptive gravity model. *New J. Phys.* **18**, 073042
382 (2016).

383 (25) Kelley, D. H. & Ouellette, N. T. Emergent dynamics of laboratory insect swarms. *Sci. Rep.*
384 **3**, 1073 (2013).

385 (26) Sinhuber, M., van der Vaart, K. & Ouellette, N. T. Response of insect swarms to dynamic
386 illumination perturbations. *J. R. Soc. Interface* **16**, 20180739 (2019).

387 (27) Takatori, S. C., Yan, W. & Brady, J. F. Swim pressure: stress generation in active matter.
388 *Phys. Rev. Lett.* **113**, 028103 (2014).

389 (28) Fodor, É., Nardini, C., Cates, M. E., Tailleur, J., Visco, P. & van Wijland, F. How far from
390 equilibrium is active matter? *Phys. Rev. Lett.* **117**, 038103 (2016).

391 (29) Ni, R., Puckett, J. G., Dufresne, E. R. & Ouellette, N. T. Intrinsic fluctuations and driven
392 response of insect swarms, *Phys. Rev. Lett.* **115**, 118104 (2015).

393 (30) Downe, A. E. R. & Caspary, V. G. The swarming behaviour of *Chironomus riparius*
394 (Diptera: Chironomidae) in the laboratory. *Can. Entomol.* **105**, 165-171 (1973).
395 (31) Tsai, R. A versatile camera calibration technique for high-accuracy 3D machine vision
396 metrology using off-the-shelf TV cameras and lenses. *IEEE J. Robot. Autom.* **RA-3**, 323-344
397 (1987).
398 (32) Ouellette, N. T., Xu, H. & Bodenschatz, E. A quantitative study of three-dimensional
399 Lagrangian particle tracking algorithms. *Exp. Fluids* **40**, 301-313 (2006).
400 (33) Puckett, J. G. & Ouellette, N. T. Determining asymptotically large population sizes in insect
401 swarms. *J. R. Soc. Interface* **11**, 20140710 (2014).

402 [\(34\) G. Vásárhelyi et al. Optimized flocking of autonomous drones in confined environments](#)
403 [Sci. Robot.](#) **3**, eaat3536 (2018).

404 [\(35\) Ni, R., Puckett, J. G., Dufresne, E. R. and Ouellette, N. T. Intrinsic fluctuations and driven](#)
405 [response of insect swarms. Phys. Rev. Lett.](#) **115**, 118104 (2015).

407 [\(35\) Fedorova, M. V. and Zhantiev, R. D. Structure and function of the Johnston's organ in](#)
408 [Fleuria lacustris Kieff. males \(Diptera, Chironomidae\). Entomol. Rev.](#) **89**, 896 (2009)

409 ~~[\(36\) G. Vásárhelyi et al. Optimized flocking of autonomous drones in confined environments](#)~~
410 ~~[Sci. Robot.](#) **3**, eaat3536 (2018)~~

411 **Acknowledgments:** This research was sponsored by the Army Research Laboratory and
412 accomplished under grant no. W911NF-16-1-0185. The views and conclusions in this document
413 are those of the authors and should not be interpreted as representing the official policies, either
414 expressed or implied, of the Army Research Laboratory or the U.S. government. K.v.d.V.
415 acknowledges support from an Early Postdoc.Mobility fellowship from the Swiss National
416 Science Foundation, and M.S. acknowledges support from the Deutsche
417 Forschungsgemeinschaft under grant no. 396632606. The work at Rothamsted forms part of the

418 Smart Crop Protection (SCP) strategic programme (BBS/OS/CP/000001) funded through the
419 Biotechnology and Biological Sciences Research Council's Industrial Strategy Challenge Fund.
420 **Author contributions:** K.v.d.V., M.S. and N.T.O. designed the experiments. K.v.d.V., M.S.,
421 and Y.F. performed the experiments and analysed the data. A.R. developed the theory. All
422 authors interpreted the data and wrote the paper.

423 **Competing interests:** The authors declare no competing interests.

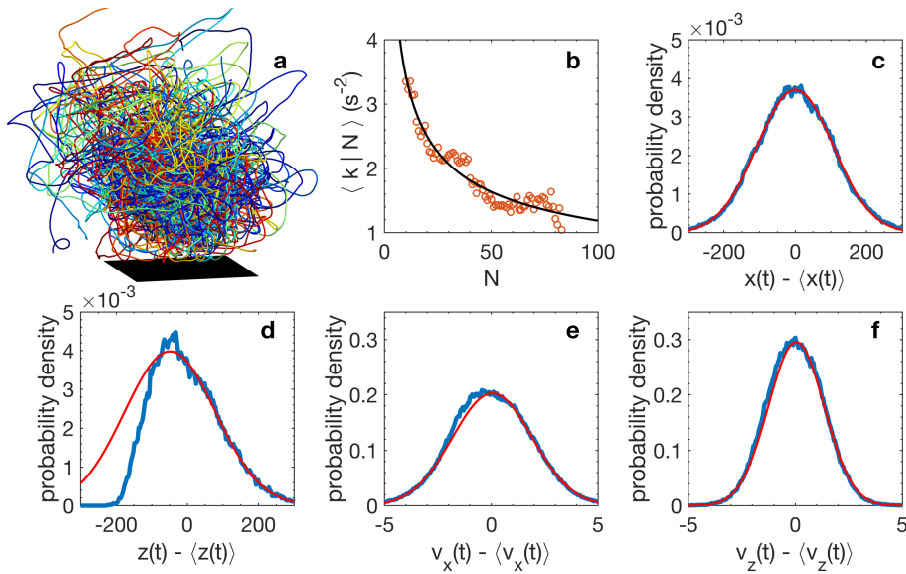
424 **Data and materials availability:** The trajectory data are available at
425 <https://doi.org/10.6084/m9.figshare.11791071.v1>

426

427

428

429 **Figures**



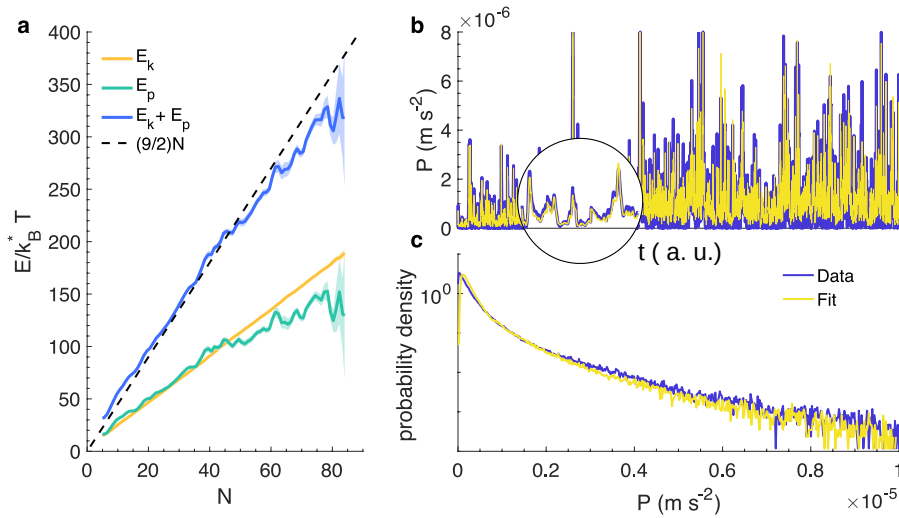
430

431

432 **Figure 1 | Swarm kinematics. a**, Trajectories (>40 s long) of individual midges (each colour
 433 corresponding to a different midge) are individually convoluted but remain spatially localized
 434 over a ground-based swarm marker (black square). **b**, Averaged spring constant $\langle k|N \rangle$ as
 435 function of the swarm size N (symbols). The black line is a power-law fit to the data. **c**,
 436 Probability density function (PDF) of midge positions in the horizontal plane (blue) along with a
 437 Gaussian fit to the data (red). **d**, PDF of midge positions in the vertical (gravity) direction (blue)
 438 and a Gaussian fit to the data (red). The deviation from Gaussianity in the vertical component of
 439 the position arises from the symmetry breaking due to the bottom floor of the experimental setup.
 440 **e,f**, PDFs of the horizontal (**e**) and vertical (**f**) midge velocities (blue) along with Gaussian fits to
 441 the data (red).

442

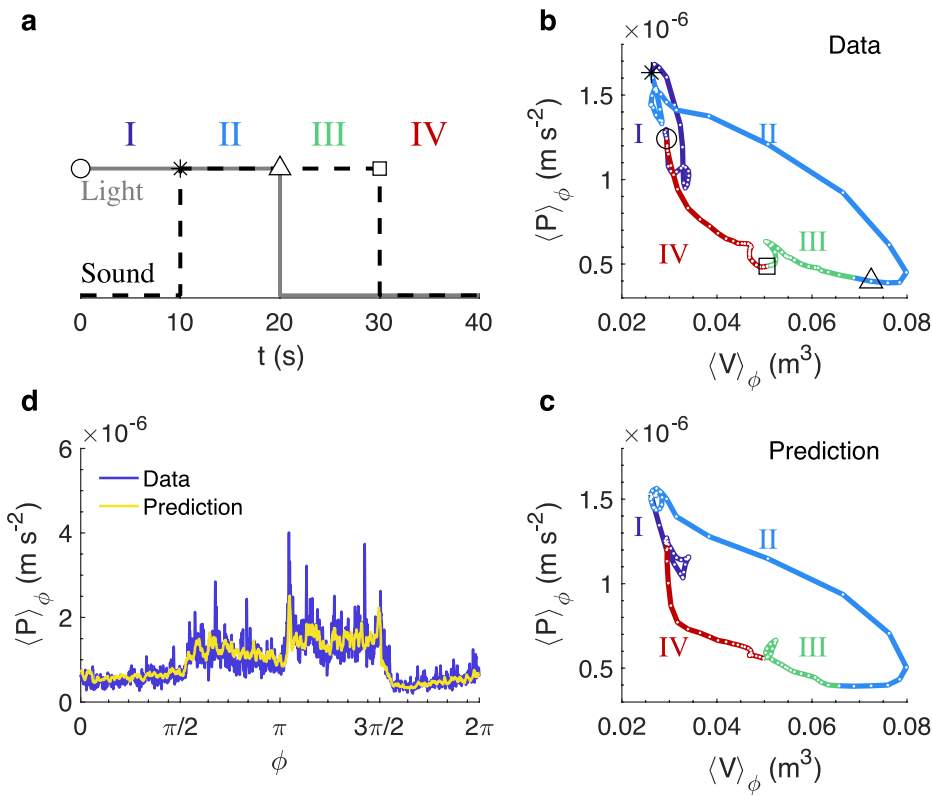
443



444

445 **Figure 2 | Equipartition and the equation of state. a**, The total energy of the system E
 446 normalized by $k_B^* T$ as a function of swarm size (blue) along with the kinetic energy E_k (yellow)

447 and potential energy E_p (blue). The total normalized energy of the system is well approximated
 448 by $(9/2)N$ (black dashed line), indicating that each individual midge contributes $(9/2)k_B^* T$ to E
 449 and thus has 9 degrees of freedom (6 after discounting the factor of $\ln 2$ in our definition of $k_B^* k$
 450 T). The deviations from that behaviour for the largest swarms can be attributed to a growing
 451 uncertainty in the energy due to the smaller number of experiments with such large swarms. **b**, A
 452 portion of our ensemble of data of the measured pressure (blue). The yellow line is the
 453 reconstruction of the pressure from our equation of state. The inset shows a zoomed-in portion of
 454 the data to highlight the quality of the reconstruction. **c**, PDF of the pressure for our entire data
 455 ensemble²³. The statistics of the directly measured pressure (blue) and reconstructed pressure
 456 from the equation of state have nearly identical statistics for the full dynamic range of the signal.
 457



459 **Figure 3 | Thermodynamic cycling of a midge swarm with $\langle N \rangle = 27$.** Schematic of the
460 perturbation cycle showing the illumination (solid) and sound (dashed) signal timings. The
461 symbols indicate the switching points identified in (b). **b,c**, Phase-averaged swarm behaviour
462 during the perturbation cycle plotted in the pressure-volume phase plane for (b) the pressure
463 signal as measured and (c) as reconstructed using our equation of state. $\langle \cdot \rangle_\phi$ denotes a phase
464 average of a quantity over a full cycle. The four different states of the perturbation signal are
465 indicated. The data has been averaged using a moving 3.5-second window for clarity. The swarm
466 behaviour moves in a closed loop in this phase plane during this cycling, as would be expected
467 for an engine in equilibrium thermodynamics, and the equation of state holds throughout even
468 though it was developed only for unperturbed swarms. **d**, Phase-averaged pressure $\langle P \rangle_\phi$ of the
469 swarm during a continuous cycle through the four light and sound states. The blue line shows the
470 directly measured pressure and the yellow line shows the reconstruction using the equation of
471 state.
472